John von Neumann Institute for Computing

The Korringa-Kohn-Rostoker (KKR) Green Function Method
I. Electronic Structure of Periodic Systems

Phivos Mavropoulos and Nikos Papanikolaou

published in

Computational Nanoscience: Do It Yourself!,
J. Grotendorst, S. Blügel, D. Marx (Eds.),
John von Neumann Institute for Computing, Jülich,
NIC Series, Vol. **31**, ISBN 3-00-017350-1, pp. 131-158, 2006.

The Korringa-Kohn-Rostoker (KKR) Green Function Method I. Electronic Structure of Periodic Systems

Phivos Mavropoulos[1] **and Nikos Papanikolaou**[2]

[1] Institute of Solid State Research
Forschungszentrum Jülich
52425 Jülich, Germany
E-mail: ph.mavropoulos@fz-juelich.de

[2] Institute of Microelectronics
NCSR Demokritos, GR-15310 Athens, Greece

The Korringa-Kohn-Rostoker (KKR) method for the calculation of the electronic structure of materials is founded on the concepts of the Green function and of multiple-scattering. In this manuscript, after a short introduction to Green functions, we present a description of single-site scattering (including anisotropic potentials) and multiple-scattering theory and the KKR equations. The KKR representation of the Green function and the algebraic Dyson equation are introduced. We then discuss the screened KKR formalism, and its advantages in the numerical effort for the calculation of layered systems. Finally we give a summary of the self-consistency algorithm for the calculation of the electronic structure.

1 Introduction and Historical Survey

The multiple-scattering method of Korringa, Kohn and Rostoker for the calculation of the electronic structure of materials was introduced in 1947 by Korringa[1] and in 1954 by Kohn and Rostoker.[2] Characteristic of this method is the use of *multiple-scattering theory* for the solution of the Schrödinger equation and the determination of the electron band structure. In such an approach, the scattering properties of each scattering center (atom) are determined in a first step and described by a scattering matrix, while the multiple-scattering by all atoms in the lattice is determined in a second step by demanding that the incident wave at each center is the sum of the outgoing waves from all other centers. In this way, a separation between the potential and geometric properties is achieved.

A further significant development of the KKR scheme came when it was reformulated as a Green function method.[3,4] Once more separating the single-site scattering problem from the multiple-scattering effects, the method is able to produce the crystal Green function efficiently by relating it to the Green function of free space via the Dyson equation. In a second step the crystal Green function can be used as a reference in order to calculate the Green function of an impurity in the crystal,[5] again via a Dyson equation. This way of solving the impurity problem is extremely efficient, avoiding the construction of huge supercells which are needed in wavefunction methods.

Chemically disordered alloys can also be treated by the KKR method within the coherent potential approximation (CPA).[7] In this approximation one defines the Green function of an average crystal medium, determined self-consistently through the condition that the concentration average of the various atom types should not produce any scattering in this medium.

The development of *screened*, or *tight-binding*, KKR was a further breakthrough for the numerical efficiency of the method.[8] Via a transformation of the reference system remote lattice sites are decoupled, and the principal layer technique allows the calculation time to scale linearly with the number of atoms. This is especially useful for layered systems (surfaces, interfaces, multilayers) and allows the study of, e.g., interlayer exchange coupling or ballistic transport through junctions.

Transport properties have also been addressed within the KKR method, since the computation Green function allows for approaches of the Kubo-Greenwood type (for diffusive transport)[9] or the Landauer-Büttiker-type (for ballistic transport).[10] Combined with the Boltzmann equation[6] the method for solving the impurity problem is also ideally suited for the calculation of transport properties in dilute metallic alloys.

In recent years, an attempt for *ab initio* calculations beyond density functional theory (DFT) has led to the development of hybrid theories which combine the local density approximation (LDA) to DFT with dynamical mean-field theory (DMFT). In these "LDA+DMFT" schemes the Green function is a central quantity, since the electron self-energy is evaluated diagrammatically and included in the propagators through a Dyson equation. Therefore the KKR Green function formalism is well suited for further development in this direction, and steps have already been taken to include DMFT in the KKR scheme.[11]

A short list of successful applications of the KKR method for electronic structure of solids, combined with density functional theory, includes bulk materials[12], surfaces[13], interfaces and tunnel junctions[14], and impurities in bulk and on surfaces.[15] Spectroscopic properties[16] and transport properties[17–19] have also been studied within this method. The KKR scheme can incorporate the Dirac equation, whenever relativistic effects become important.[20]

Since the KKR method is concerned with the propagation of waves through an array of scatterers, its applications are not restricted to the field of the electronic structure of solids. The propagation of, e.g., electromagnetic waves in photonic crystals,[21] or the propagation of elastic waves through photonic crystals[22] can be efficiently described by multiple-scattering theory, and the useful features of KKR, such as the CPA, can be also generalized for these cases.[23]

In this manuscript we present the basics of the KKR formalism. After a general introduction to Green functions in Section 2, we give an analysis of the single-site scattering problem in Section 3. We continue with a detailed presentation of multiple-scattering theory (Section 4), where the basic ideas are given independently of a Green function formulation; we then attend to the KKR representation of the Green function in Section 5. Details on the single-site scattering problem by non-spherical potentials are given in Section 6, while the method for total energy calculations is summarized in Section 7. We carry on with the basics of screened KKR in Section 8, and briefly show how to calculate surfaces or interfaces in Section 9. Finally, we discuss the self-consistency procedure, including the idea of complex-energy contour integration, in Section 10. The reader is assumed to know the basics of DFT, of the LDA, and of electronic structure calculations. These are not essential for the multiple-scattering formalism, but become important in Sections 7 and 10. The solution of the impurity problem within the KKR Green function method is described in the manuscript of Peter H. Dederichs (see page 279).

2 Definition and General Properties of the Green Function

In this section we give a brief introduction to Green functions in scattering problems. The purpose of the introduction is to remind of the concepts and formulas which will be used in the subsequent sections. For more details, including mathematical rigor, we refer to the literature, e.g., to the book by Newton[24] or by Economou.[25]

2.1 Time-Dependent Green Functions

Consider an electron under the influence of a potential $V(\vec{r})$. The Hamiltonian is

$$H = -\nabla^2 + V(\vec{r}) = H_{\text{free}} + V(\vec{r}). \tag{1}$$

Here, and in the following, we use atomic units ($\hbar = 1$, $m_{\text{e}} = \frac{1}{2}$, $e = -\sqrt{2}$). The time-dependent Schrödinger equation, determining the time evolution of the electron wavefunction $\psi(t)$, is

$$i\frac{\partial}{\partial t}\psi(t) = H\psi(t) \tag{2}$$

with formal solution

$$\psi(t) = e^{-iHt}\psi(0), \tag{3}$$

and with $\psi(0)$ representing the wavepacket preparation as an initial condition. The quantity $U(t) = e^{-iHt}$ is the time evolution operator in quantum mechanics.

Corresponding to the Schrödinger equation, we define now two propagators, the *retarded Green function* $G^R(t)$ and the *advanced Green function* $G^A(t)$, as

$$\left(i\frac{\partial}{\partial t} - H\right) G^{R,A}(t) = \delta(t) \tag{4}$$

with boundary conditions

$$G^R(t) = 0 \qquad t < 0 \tag{5}$$

$$G^A(t) = 0 \qquad t > 0. \tag{6}$$

The formal solution of these equations is

$$G^R(t) = \begin{cases} -ie^{-iHt} & t > 0 \\ 0 & t < 0 \end{cases} \tag{7}$$

$$G^A(t) = \begin{cases} 0 & t > 0 \\ ie^{-iHt} & t < 0 \end{cases}. \tag{8}$$

Evidently, the Green functions coincide, up to a factor, with the time evolution operator; $G^R(t)$ is used to propagate the wavefunction forward in time, and $G^A(t)$ to propagate the wavefunction backward in time:

$$\psi(t) = \ iG^R(t-t')\psi(t') \qquad t' < t \tag{9}$$

$$\psi(t) = -iG^A(t-t')\psi(t') \qquad t < t'. \tag{10}$$

In the following we shall restrict the discussion to the retarded Green function G^R and drop the index R.

Given a perturbing potential $\Delta V(\vec{r})$ added to a Hamiltonian H_0, it follows from Eq. (5) that the Green function G_1 corresponding to the new Hamiltonian $H_1 = H_0 + \Delta V$ is related to the Green function G_0 corresponding to H_0 via the Dyson integral equation

$$G_1(t) = G_0(t) + \int_0^t G_0(t-t')\,\Delta V\,G_1(t')\,dt'. \tag{11}$$

Furthermore, it can be proven that an incoming wavepacket ψ_0, which without the interaction with ΔV would evolve as $\psi_0(t)$, evolves into the wavefunction $\psi(t)$ as

$$\psi(t) = \psi_0(t) + \int_{-\infty}^t G_0(t-t')\,\Delta V\,\psi(t')\,dt'; \tag{12}$$

this is the *Lippmann-Schwinger equation*.

2.2 Energy-Dependent Green Functions

A Fourier transform of the Green function,

$$G(E) = \int_{-\infty}^{\infty} G(t)\,e^{i(E+i\varepsilon)t}\,dt \tag{13}$$

results in the formal solution

$$G(E) = (E + i\varepsilon - H)^{-1}. \tag{14}$$

Here, ε is a positive real number, to be taken in the end to the limit $\varepsilon \to 0$, which ensures convergence of the integral in Eq. (13) for $t \to \infty$. More generally, one may define the (time-independent) Green function as the resolvent of the time-independent Schrödinger equation, via the operator equation

$$G(E) = (E - H)^{-1} \tag{15}$$

for an arbitrary complex energy E (as long as $(E - H)$ can be inverted). The singularities of $G(E)$ determine the eigenvalue spectrum; in particular, $G(E)$ has poles at the eigenenergies of the bound states, and a branch cut along the energies of the continuous spectrum. For $\mathrm{Im}E > 0$, $G(E)$ is an analytical function of E. In terms of a complete set of eigenfunctions of H, $|\psi_i\rangle$, corresponding to eigenvalues ϵ_i, the following spectral representation can be obtained:

$$G(E) = \sum_i \frac{|\psi_i\rangle\langle\psi_i|}{E - \epsilon_i}. \tag{16}$$

Represented in real space, the above equation becomes

$$G(\vec{r},\vec{r}\,';E) = \sum_i \frac{\psi_i(\vec{r})\,\psi_i^*(\vec{r}\,')}{E - \epsilon_i} \tag{17}$$

representing, in the limit of $\mathrm{Im}E = \varepsilon \to 0^+$, an outgoing wave at $\vec{r}$ with a source term at $\vec{r}\,'$. From the above equation one can see that the imaginary part of G is directly related to the spectrally- and space-resolved density of states $n(\vec{r};E)$ (for real E):

$$n(\vec{r};E) = -\frac{1}{\pi}\mathrm{Im}\,G(\vec{r},\vec{r};E). \tag{18}$$

This follows from the Dirac identity,

$$\int_{-\infty}^{\infty} \frac{f(x)}{x - x_0 \pm i\varepsilon} dx = P\left(\int_{-\infty}^{\infty} \frac{f(x)}{x - x_0} dx\right) \mp i\pi f(x_0) \tag{19}$$

where P stands for the Cauchy principal part of the integral. One can deduce from Eq. (18) an expression for the spectral density of states,

$$n(E) = -\frac{1}{\pi} \mathrm{Im} \int G(\vec{r}, \vec{r}; E)\, d^3r = -\frac{1}{\pi} \mathrm{Im}\,\mathrm{Tr}\, G(E), \tag{20}$$

where the last step stresses that the trace of the operator $G(E)$ can be taken in any basis, not just in real-space representation. On the other hand, the charge density is found as an integral of $n(\vec{r}; E)$ over the energies up to the Fermi level:[a]

$$\rho(\vec{r}) = -\frac{1}{\pi} \mathrm{Im} \int_{-\infty}^{E_F} G(\vec{r}, \vec{r}; E)\, dE = -\frac{1}{\pi} \mathrm{Im} \int_{-\infty}^{E_F} \mathrm{Tr}\left(\hat{r}\, G(E)\right)\, dE \tag{21}$$

with $\hat{r} = |\vec{r}\rangle \delta(\vec{r} - \vec{r}\,')\langle \vec{r}\,'|$ is the position operator.

In general, from the spectral representation (Eq. (16)) it follows that the expectation value of any physical quantity, represented by an operator $\hat{A}$, can be harvested via the relation

$$\langle A \rangle = -\frac{1}{\pi} \mathrm{Im} \int_{-\infty}^{E_F} \mathrm{Tr}\left[\hat{A}\, G(E)\right]\, dE. \tag{22}$$

Therefore, the Green function contains all information which is given by the eigenfunctions. If the Green function can be computed, then all physical properties of the system can be found.

2.3 Relation between Perturbed and Unperturbed System. The T-Matrix

The time-dependent Dyson equation (11) has its energy-dependent counterpart. Given from Eq. (15) that for the reference system $G_0^{-1}(E) = E - H_0$, while for the perturbed system $G_1^{-1}(E) = E - (H_0 + \Delta V)$, we conclude that the two Green functions are connected via

$$G_1^{-1}(E) = G_0^{-1}(E) - \Delta V. \tag{23}$$

The Dyson equation can be rewritten in the following forms (which can be directly verified by substitution in Eq. (23)):

$$G_1(E) = [1 - G_0(E)\, \Delta V]^{-1}\, G_0(E) \tag{24}$$

$$= G_0(E)\, [1 - \Delta V\, G_0(E)]^{-1} \tag{25}$$

$$= G_0(E) + G_0(E)\, \Delta V\, G_1(E). \tag{26}$$

The last expression, although not in a closed form, reminds of expression in Eq. (11) and allows for an interpretation of the Dyson equation via multiple-scattering events by the perturbing potential ΔV if we expand G_1 in the right-hand side:

$$G_1(E) = G_0(E) + G_0(E)\, \Delta V\, G_0(E) + G_0(E)\, \Delta V G_0(E)\, \Delta V\, G_0(E) + \cdots\,; \tag{27}$$

[a] This is of course valid for fermions at $T = 0$; otherwise a convolution with the Fermi function, or the appropriate distribution function, is needed.

this is the analogue of a Born series expansion for the Green function.

Also the Lippmann-Schwinger equation (12) has a time-independent counterpart. Observing that the Schrödinger equation for the perturbed system can be written as

$$(E - H)\,|\psi_1\rangle = \Delta V\,|\psi_1\rangle, \tag{28}$$

we can verify by substitution that the solution $|\psi_1\rangle$ can be written in terms of the unperturbed eigenstates $|\psi_0\rangle$ as

$$|\psi_1\rangle = |\psi_0\rangle + G_0(E)\,\Delta V\,|\psi_1\rangle. \tag{29}$$

Expanding $|\psi_1\rangle$ on the right-hand side of this Lippmann-Schwinger equation leads to the Born series

$$|\psi_1\rangle = |\psi_0\rangle + G_0(E)\,\Delta V\,|\psi_0\rangle + G_0(E)\,\Delta V\,G_0(E)\,\Delta V\,|\psi_0\rangle + \cdots. \tag{30}$$

In the case that E does not belong to the spectrum of the unperturbed Hamiltonian H, $|\psi_0\rangle = 0$ and we have

$$|\psi_1\rangle = G_0(E)\,\Delta V\,|\psi_1\rangle. \tag{31}$$

This expression can be used to obtain the discrete spectrum of H_1.

We now introduce the transition matrix, or T-matrix, of a scattering system. It relates the states $|\psi_1\rangle$ of the perturbed Hamiltonian to the states $|\psi_0\rangle$ of the unperturbed system via the defining equation

$$\Delta V|\psi_1\rangle = T(E)|\psi_0\rangle. \tag{32}$$

In terms of the T-matrix the Lippmann-Schwinger equation (29) is written as

$$|\psi_1\rangle = |\psi_0\rangle + G_0(E)\,T(E)\,|\psi_0\rangle, \tag{33}$$

the Dyson equation (26) as

$$G_1(E) = G_0(E) + G_0(E)\,T(E)\,G_0(E), \tag{34}$$

while the following relations can be easily verified:

$$T(E) = \Delta V\,[1 - G_0(E)\Delta V]^{-1} \tag{35}$$

$$= [1 - \Delta V\,G_0(E)]^{-1}\,\Delta V \tag{36}$$

$$= \Delta V + \Delta V\,G_0(E)\,T(E). \tag{37}$$

Expanding the right-hand side of the last equation leads once more to a Born series:

$$T(E) = \Delta V + \Delta V\,G_0(E)\,\Delta V + \Delta V\,G_0(E)\,\Delta V\,G_0(E)\,\Delta V + \cdots, \tag{38}$$

while for small perturbations we are led to the first-order Born approximation, $T \simeq \Delta V$.

Via the T-matrix one can express the change in the integrated density of states, $\Delta N(E)$, between the perturbed and the unperturbed system. From Eq. (20) it follows that the change in the density of states is

$$\Delta n(E) \equiv n_1(E) - n_0(E) = -\frac{1}{\pi}\mathrm{Im}\mathrm{Tr}\,[G_1(E) - G_0(E)]\,. \tag{39}$$

Eq. (15) gives us, on the other hand, the identity $G = \partial(\ln G^{-1})/\partial E$. Combining this with (39) we proceed as

$$\Delta n(E) = -\frac{1}{\pi}\mathrm{Im}\mathrm{Tr}\frac{\partial}{\partial E}\left[\ln G_1^{-1} - \ln G_0^{-1}\right] = -\frac{1}{\pi}\mathrm{Im}\mathrm{Tr}\frac{\partial}{\partial E}\ln\left[G_0\, G_1^{-1}\right] \quad (40)$$

$$= -\frac{1}{\pi}\mathrm{Im}\frac{\partial}{\partial E}\mathrm{Tr}\ln\left[1 - G_0\,\Delta V\right] \quad (41)$$

$$= -\frac{1}{\pi}\mathrm{Im}\frac{\partial}{\partial E}\mathrm{Tr}\ln\left[T^{-1}\,\Delta V\right]. \quad (42)$$

In the last two steps we used the Dyson equation (24) and the property (Eq. (35)) of the T-matrix. The integrated change in the density of states is thus

$$\Delta N(E) = \int_{-\infty}^{E}\Delta n(E')\,dE' = -\frac{1}{\pi}\mathrm{Im}\mathrm{Tr}\ln\left[T^{-1}(E)\,\Delta V\right]_{-\infty}^{E}. \quad (43)$$

By splitting the logarithm as $\ln(T^{-1}(E)\,\Delta V) = \ln T^{-1}(E) + \ln\Delta V$ we see that the contribution of ΔV drops out.[b] Since the lower integration limit ($-\infty$) is below the spectrum of the Hamiltonian, it also gives no contribution. We are thus left with the result

$$\Delta N(E) = \frac{1}{\pi}\mathrm{Im}\mathrm{Tr}\ln T(E). \quad (44)$$

In the following section we will associate the perturbation ΔV with a spherically symmetric potential of finite range in free space. Then we have a single-site scattering problem, and we will denote the T-matrix as t; in angular-momentum representation it is diagonal and its elements are related to the scattering phase shifts $\delta_l(E)$ via

$$t_l = -\frac{1}{\sqrt{E}}\sin(\delta_l(E))e^{i\delta_l(E)}.$$

In this special case, Eq. (44) becomes

$$\Delta N(E) = \frac{1}{\pi}\sum_l (2l+1)\delta_l(E). \quad (46)$$

If the scattering potential represents an impurity in a free-electron host, then the integrated difference of density of states up to the Fermi level, $\Delta N(E_F)$, must be equal to the additional charge introduced by the impurity, $Z_{\mathrm{imp}} - Z_{\mathrm{host}}$. This is expressed by the *Friedel sum rule*. Including a factor 2 for the spin degeneracy, the rule reads:

$$Z_{\mathrm{imp}} - Z_{\mathrm{host}} = \frac{2}{\pi}\sum_l (2l+1)\delta_l(E_F). \quad (47)$$

3 Single-Site Scattering

We turn now to the scattering problem of a spherical atomic potential embedded in free space (actually in an environment of constant potential). The reference system is thus a free-electron system (where the Hamiltonian contains only the kinetic energy term, and

[b] This is because ΔV does not depend on the energy; in systems where the perturbation is energy-dependent, e.g., a self-energy, it must be accounted for.

the eigenfunctions are plain waves). The Green function of a free-electron system has the form[24, 25]

$$g(\vec{r},\vec{r}\,';E) = -\frac{1}{4\pi}\,\frac{e^{ik|\vec{r}-\vec{r}\,'|}}{|\vec{r}-\vec{r}\,'|}. \tag{48}$$

with $k = \sqrt{E}$. In the case of scattering by a central potential, it is useful to work in angular-momentum representation. We therefore represent an incoming plain wave as

$$\psi^{\rm inc}_{\vec{k}}(\vec{r}) = e^{i\vec{k}\vec{r}} = \sum_L 4\pi i^l\, j_l(\sqrt{E}r)\, Y_L(\vec{r})\, Y_L(\vec{k}) \tag{49}$$

where j_l is the spherical Bessel function, while Y_L are the real spherical harmonics (see Appendix 10). We use the combined index $L := (l,m)$, where l and m are angular momentum indexes. On the other hand, the free-space Green function (48) can be expanded as:

$$g(\vec{r},\vec{r}\,';E) = \sum_L Y_L(\vec{r})\, g_l(r,r';E)\, Y_L(\vec{r}\,') \tag{50}$$

with

$$g_l(r,r';E) = -i\sqrt{E}\, j_l(\sqrt{E}r_<)\, h_l(\sqrt{E}r_>), \tag{51}$$

where $h_l = j_l + i n_l$ are spherical Hankel functions, n_l are spherical Neumann functions,[26] while $r_<$ ($r_>$) is the smaller (bigger) of the radii r and r'. The Bessel functions $j_l(x)$ are finite as $x \to 0$, while $h_l(x)$ and $n_l(x)$ are diverging as $x \to 0$.

Suppose now that there is a scattering potential of finite range, of the form

$$V(\vec{r}) = \begin{cases} V(r) & r \le S \\ 0 & r > S. \end{cases} \tag{52}$$

Then the radial wavefunctions $R_l(r;E)$ satisfy the radial Schrödinger equation

$$\left[-\frac{1}{r}\frac{\partial^2}{\partial r^2}r + \frac{l(l+1)}{r^2} + V(r) - E\right] R_l(r;E) = 0. \tag{53}$$

The asymptotic form of $R_l(r;E)$ for $r \to \infty$ is

$$R_l(r;E) \to \frac{A_l}{\sqrt{E}r}\sin\left(\sqrt{E}r - \frac{l\pi}{2} + \delta_l(E)\right) \tag{54}$$

where A_l is independent of r and $\delta_l(E)$ is the phase shift with respect to the wavefunction for vanishing potential.

For $r > S$, $V(r) = 0$ and the general solution of the radial equation is a sum of two linearly independent special solutions:

$$R_l(r;E) = B_l\, j_l(\sqrt{E}r) + C_l\, n_l(\sqrt{E}r) \tag{55}$$

where B_l and C_l are constants. Using the asymptotic form of Bessel functions,

$$\lim_{x\to\infty} j_l(x) = \frac{1}{x}\sin(x - l\pi/2) \tag{56}$$

$$\lim_{x\to\infty} n_l(x) = -\frac{1}{x}\cos(x - l\pi/2) \tag{57}$$

together with Eqs. (54) and (55), we obtain

$$R_l(r;E) = A_l\left(j_l(\sqrt{E}r)\cos\delta_l - n_l(\sqrt{E}r)\sin\delta_l\right) \quad \text{for } r > S. \tag{58}$$

On the other hand, the Lippmann-Schwinger equation gives

$$R_l(r;E) = j_l(\sqrt{E}r) + \int_0^S g_l(r,r';E)\,V(r')\,R_l(r';E)\,r'^2\,dr' \tag{59}$$

which, using Eq. (51), yields for $r > S$:

$$R_l(r;E) = j_l(\sqrt{E}r) - ih_l(\sqrt{E}r)\sqrt{E}\int_0^S j_l(\sqrt{E}r')\,V(r')\,R_l(r';E)\,r'^2\,dr'. \tag{60}$$

The integral is just the t-matrix element in angular-momentum representation (see Eq. (32)),

$$t_l(E) = \int_0^S j_l(\sqrt{E}r)\,V(r)\,R_l(r;E)\,r^2 dr, \tag{61}$$

so that we obtain

$$R_l(r;E) = j_l(\sqrt{E}r) - i\sqrt{E}\,t_l(E)\,h_l(\sqrt{E}r) \quad (r > S) \tag{62}$$

with the t-matrix related to the phase shift by (cf. (58))

$$t_l(E) = -\frac{1}{\sqrt{E}}\sin\delta_l(E)\,e^{i\delta_l(E)}. \tag{63}$$

An incoming wave can be expanded in Bessel functions and spherical harmonics as (cf. (49))

$$\psi_{\vec{k}}^{\text{inc}}(\vec{r}) = \sum_L a_{\vec{k}L}^0 j_l(\sqrt{E}r)\,Y_L(\vec{r}) \quad (\text{for } r > S). \tag{64}$$

The scattered wave can be expanded analogously as:

$$\psi_{\vec{k}}^{\text{sc}}(\vec{r}) = \sum_L a_{\vec{k}L}^{\text{sc}}\,j_l(\sqrt{E}r)\,Y_L(\vec{r}) \quad (\text{for } r > S). \tag{65}$$

Within the range S of the potential we have

$$\psi_{\vec{k}}(\vec{r}) = \sum_L a_{\vec{k}L}\,R_l(r;E)\,Y_L(\vec{r}) \tag{66}$$

with the boundary conditions of R_l given by (62). From the continuity of the wavefunction at $r = S$, we obtain then

$$a_{\vec{k}L}^{\text{sc}} = -i\sqrt{E}\,t_l(E)\,a_{\vec{k}L}^0. \tag{67}$$

Finally, we give without proof the Green function for the scattering problem by a central potential. It can be written as the product of two linearly independent solutions, R_l (regular, i.e., converging at $r \to 0$) and H_l (irregular, i.e., diverging at $r \to 0$), of the radial equation:

$$\begin{aligned} G(\vec{r},\vec{r}\,';E) &= -i\sqrt{E}\sum_L R_l(r_<;E)H_l(r_>;E)\,Y_L(\vec{r})\,Y_L(\vec{r}\,') \\ &\equiv \sum_L G_l(r,r';E)\,Y_L(\vec{r})\,Y_L(\vec{r}\,'). \end{aligned} \tag{68}$$

The boundary conditions of R_l are given by Eq. (62). In order to find the boundary conditions of H_l we use the identity (34) $G_l = g_l + g_l\, t_l\, g_l$ with g_l given by (51) and obtain

$$H_l(r;E) = h_l(\sqrt{E}r) \quad (r > S). \tag{69}$$

In practice, we integrate Eq. (53) numerically outwards from the origin to $r = S$ in order to obtain R_l. At $r = S$ the requirement for continuity of the logarithmic derivative yields the t-matrix elements. Analogously, a numerical integration inwards yields the diverging radial wavefunction H_l, given the boundary condition (69) at $r = S$.

4 Multiple-Scattering Theory

In the previous section we discussed the solution of the scattering problem for an isolated scattering potential. In this section we will extend the study to a set of scatterers. At this point we assume the *muffin-tin* (MT) approximation to the scattering potential, according to which the potential is spherically symmetric around each scattering center (atomic site), within a sphere of radius R_{MT}, and constant otherwise; the spheres can be touching each other, but are assumed to be non-overlapping.[c] The theory presented here is based on the bookkeeping of the scattering amplitudes in a periodic array of scatterers, so that a secular equation connecting the amplitudes of incoming and outgoing waves emerges. The procedure leads to the KKR equations for the band structure of periodic crystals. Although the procedure is not necessary for the KKR Green function theory, it provides physical insight to the ideas founding multiple-scattering theory, used in many wave-scattering problems even when a Green function is not introduced. The connection to the KKR representation of the Green function will be done in the next section.

Assume a periodic structure of MT potentials, centered at lattice sites $\vec{R}^n$. The constant potential in the interstitial can be taken to be zero. An outgoing wave from site $\vec{R}^n$ can be expanded in incoming waves at site $\vec{R}^{n'}$ by employing a theorem for the transformation of Hankel functions:

$$h_L(\vec{r}\,' + \vec{R}^{n'} - \vec{R}^n; E) = \frac{i}{\sqrt{E}} \sum_{L'} g^{nn'}_{LL'}(E)\, j_{L'}(\vec{r}\,'; E), \tag{70}$$

where we have used the abbreviations

$$j_L(\vec{r}\,'; E) = j_l(\sqrt{E}r)\, Y_L(\vec{r}) \quad \text{and} \quad h_L(\vec{r}\,'; E) = h_l(\sqrt{E}r)\, Y_L(\vec{r}). \tag{71}$$

The expansion coefficients, also called *structure constants*, are given by

$$g^{nn'}_{LL'}(E) = -(1 - \delta_{nn'})\, 4\pi i \sqrt{E} \sum_{L''} i^{l-l'+l''} C_{LL'L''}\, h_{L''}(\vec{R}^n - \vec{R}^{n'}; E) \tag{72}$$

where the Gaunt coefficients

$$C_{LL'L''} = \int d\Omega\, Y_L(\vec{r})\, Y_{L'}(\vec{r})\, Y_{L''}(\vec{r}) \tag{73}$$

[c] In Section 6 we will see how the method can be extended to the general case of non-spherical site-centered potentials (the so-called *full-potential* problem).

have been introduced. The summation in Eq. (73) includes a finite number of terms, since the Gaunt coefficients vanish for $l'' > l' + l$. Using the above expansions, the free-electron Green function can be cast in the form:

$$g(\vec{r}+\vec{R}^n, \vec{r}\,'+\vec{R}^{n'}; E) = -\frac{1}{4\pi}\frac{e^{ik|\vec{r}+\vec{R}^n-\vec{r}\,'-\vec{R}^{n'}|}}{|\vec{r}+\vec{R}^n-\vec{r}\,'-\vec{R}^{n'}|}$$
$$= -i\sqrt{E}\sum_L j_L(\vec{r}_<;E)\,h_L(\vec{r}_>;E) + \sum_{LL'} j_L(\vec{r};E)\,g^{nn'}_{LL'}(E)\,j_{L'}(\vec{r}\,';E)\ . \qquad (74)$$

We proceed by considering an *outgoing* wave in the interstitial, after a scattering event by a potential at $\vec{R}^n$. It has the form

$$\psi^{\mathrm{sc}\,(n)}_{\vec{k}}(\vec{r}) = \sum_L b^{\mathrm{sc}\,(n)}_{\vec{k}L}\,h_L(\vec{r};E). \qquad (75)$$

The same wave can be resolved as an *incoming* wave at a different center $\vec{R}^{n'}$ via

$$\psi^{\mathrm{inc}\,(n')}_{\vec{k}}(\vec{r}\,') = \sum_L b^{(n')}_{\vec{k}L}\,j_L(\vec{r}\,';E). \qquad (76)$$

Thus a wave scattered at site n can be expressed as incoming to site n':

$$\sum_L b^{\mathrm{sc}\,(n)}_{\vec{k}L}\,h_L(\vec{r}\,'+\vec{R}^{n'}-\vec{R}^n;E) = \sum_L b^{(n')}_{\vec{k}L}\,j_L(\vec{r}\,';E). \qquad (77)$$

Using the identity in Eq. (70) we find

$$b^{(n')}_{\vec{k}L} = \frac{i}{\sqrt{E}}\sum_{L'} g^{nn'}_{LL'}\,b^{\mathrm{sc}\,(n')}_{\vec{k}L'}\ . \qquad (78)$$

Given the periodicity of the crystal lattice, we employ the Bloch condition according to which the amplitude of a scattered wave at position $\vec{R}^n$ differs from the amplitude of a scattered wave at position $\vec{R}^{n'}$ by a phase factor of $\exp(i\vec{k}\cdot(\vec{R}^n-\vec{R}^{n'}))$. The amplitude of the *total incoming wave* at the scatterer $\vec{R}^{n'}$, originating from all other identical scatterers, can therefore be written as

$$c^{(n')}_{\vec{k}L} = \frac{i}{\sqrt{E}}\sum_{L'}\sum_{n\neq n'} g^{nn'}_{LL'}(E)\,e^{i\vec{k}\cdot(\vec{R}^n-\vec{R}^{n'})}\,c^{\mathrm{sc}(n')}_{\vec{k}L'} = \frac{i}{\sqrt{E}}\sum_{L'} g_{LL'}(\vec{k};E)\,c^{\mathrm{sc}(n')}_{\vec{k}L'}. \qquad (79)$$

The quantities c and c^{sc} are the expansion coefficients for the total incoming and scattered wave, respectively, while

$$g_{LL'}(\vec{k};E) = \sum_{n\neq n'} g^{nn'}_{LL'}(E)e^{i\vec{k}\cdot(\vec{R}^n-\vec{R}^{n'})} \qquad (80)$$

is the Fourier transform of $g^{nn'}_{LL'}(E)$. The KKR structure constants $g_{LL'}(\vec{k};E)$ (and $g^{nn'}_{LL'}(E)$) depend only on the geometry of the lattice and not on the scattering potential.[d]

The total scattered wave from a scatterer at lattice site n' is connected to the total incoming wave at that site via the t-matrix, with elements $t_l(E)$. In the presence of an

[d]Note that the calculation of $g_{LL'}(\vec{k};E)$ demands a cumbersome Ewald summation, because the real-space $g^{nn'}_{LL'}(E)$ does not fall off fast enough in real space. Alternatively, one can use the tight-binding KKR formalism, presented in Section 8.

external incoming wave (from outside the crystal) of amplitude $a^0_{\vec{k}L}$, the total incoming wave at some site consists of the external one plus the waves scattered from all other lattice sites, so that:

$$c^{\mathrm{sc}(n')}_{\vec{k}L} = -i\sqrt{E}\, t_l(E)\, \left(a^0_{\vec{k}L} + c^{(n')}_{\vec{k}L}\right). \tag{81}$$

Combining Eqs. (81) and (79), we arrive at the following system of equations:

$$a^0_{\vec{k}L} = \sum_{L'} \left(\delta_{LL'} - g_{LL'}(\vec{k};E)\, t_{l'}(E)\right) \frac{i}{\sqrt{E}}\, t^{-1}_{l'}(E)\, c^{\mathrm{sc}(n')}_{\vec{k}L'}. \tag{82}$$

In the absence of an external incoming wave, these are rewritten as

$$\sum_{L'} \left(\delta_{LL'} - g_{LL'}(\vec{k};E)\, t_{l'}(E)\right) c^{(n')}_{\vec{k}L'} = 0. \tag{83}$$

The electronic eigenvalues in a crystal are given by the solutions of (83), i.e., in the absence of an external wave. In order to have non-trivial solutions of system (83), the necessary and sufficient condition is that the determinant vanishes:

$$\mathrm{Det}\left[\delta_{LL'} - g_{LL'}(\vec{k};E)\, t_{l'}(E)\right] = 0. \tag{84}$$

This is the KKR secular equation, giving the energy band structure $E(\vec{k})$ of periodic crystals.

The total wavefunction in the interstitial around a scatterer n is given by the sum of the incoming and scattered waves, Eqs. (75) and (76). Using Eqs. (81) and (83) we arrive at the form

$$\psi_{\vec{k}}(\vec{r} + \vec{R}^n) = \sum_L c^{(n)}_{\vec{k}L} \left[j_L(\vec{r};E) - i\sqrt{E}\, h_L(\vec{r};E)\right] \quad r \geq R_{\mathrm{MT}}. \tag{85}$$

Each component L of the wavefunction has thus the form of $R_L(\vec{r};E) = R_l(r;E)Y_L(\vec{r})$ of Eq. (62) for $r \geq S$. We are led therefore to the following form of the Bloch wavefunction in the crystal:

$$\psi_{\vec{k}}(\vec{r} + \vec{R}^n) = \sum_L c^{(n)}_{\vec{k}L}\, R_L(\vec{r};E); \tag{86}$$

Bloch's theorem implies

$$c^{(n)}_{\vec{k}L} = e^{i\vec{k}\cdot\vec{R}^n}\; c^{(0)}_{\vec{k}L}. \tag{87}$$

The coefficients $c^{(n)}_{\vec{k}L}$ can be viewed as the matrix elements of a unitary transformation between the $\vec{k}$ and (L,n) representations. The orthogonality of the bases implies:

$$\sum_{n,L} c^{(n)*}_{\vec{k}L}\, c^{(n)}_{\vec{k}'L} = \delta_{\vec{k}\vec{k}'} \tag{88}$$

$$\sum_{\vec{k}} c^{(n)*}_{\vec{k}L}\, c^{(n')}_{\vec{k}L'} = \delta_{nn'}\delta_{LL'}. \tag{89}$$

5 KKR Representation of the Green Function

We now turn to the description of the KKR Green function method, by introducing the KKR representation of the Green function and the Dyson equation.

Consider the Green function of a periodic array of spherically symmetric, non-overlapping potentials. The potential is given by

$$V(\vec{r}+\vec{R}^n) = V^n(r) \tag{90}$$

and the Green function is defined via

$$\left(-\nabla^2 + V^n(r) - E\right) G(\vec{r}+\vec{R}^n, \vec{r}\,' + \vec{R}^{n'}; E) = -\delta_{nn'}\delta(\vec{r}-\vec{r}\,') \,. \tag{91}$$

For $n \neq n'$ the Green function satisfies the homogeneous Schrödinger equation and can be expanded in the regular solutions of the Schrödinger equation $R^n_L(\vec{r};E)$ and $R^{n'}_L(\vec{r};E)$. In the muffin-tin approximation (see equation (52)), these are simply given by $R^n_L(\vec{r};E) = R^n_l(r;E)Y_L(\vec{r})$ (see equation (53)), while in the full-potential case a more cumbersome calculation is needed (see Section 6). For $n = n'$ we actually have the Green function for a central potential as in Eq. (68), but with a boundary condition of back-scattering by all other potentials in the crystal. In the end, the Green function is a sum of the general solution of the homogeneous equation corresponding to Eq. (91), plus a special solution of the inhomogeneous equation (91). In the mixed site-angular-momentum representation, the Green function is finally expanded as:

$$\begin{aligned} &G(\vec{r}+\vec{R}^n, \vec{r}\,' + \vec{R}^{n'}; E) = \\ &-i\sqrt{E}\sum_L R^n_L(\vec{r}_<;E)\, H^n_L(\vec{r}_>;E)\,\delta_{nn'} + \sum_{LL'} R^n_L(\vec{r};E)\, G^{nn'}_{LL'}(E)\, R^{n'}_{L'}(\vec{r}\,';E), \end{aligned} \tag{92}$$

where we have used the abbreviation $H^n_L(\vec{r};E) = H^n_l(r;E)Y_L(\vec{r})$ for the irregular solution of the radial equation at the atomic cell n. The coefficients $G^{nn'}_{LL'}(E)$ are called *structural Green functions*, and are at the moment unknown quantities to be calculated by use of the Dyson equation. This, taking free space as the unperturbed system, is:

$$\begin{aligned} &G(\vec{r}+\vec{R}^n, \vec{r}\,' + \vec{R}^{n'}; E) = g(\vec{r}+\vec{R}^n, \vec{r}\,' + \vec{R}^{n'}; E) + \\ &\sum_{n''}\int d^3r'' g(\vec{r}+\vec{R}^n, \vec{r}\,'' + \vec{R}^{n''}; E)\, V^{n''}(r'')\, G(\vec{r}\,''+\vec{R}^{n''}, \vec{r}\,' + \vec{R}^{n'}; E) \,. \end{aligned} \tag{93}$$

By substituting the expansions Eqs. (74) and (92) into Eq. (93), one can arrive, after some algebra,[7] at the following *algebraic Dyson equation* determining the structural Green functions:

$$G^{nn'}_{LL'}(E) = g^{nn'}_{LL'}(E) + \sum_{n'',L''} g^{nn''}_{LL''}(E)\, t^{n''}_{l''}(E)\, G^{n''n'}_{L''L'}(E) \tag{94}$$

where the t-matrix enters, instead of the potential which appears in the normal Dyson equation. The physical significance of this equation becomes clearer if we expand the sum on the right-hand side, whence we obtain:

$$G^{nn'}_{LL'} = g^{nn'}_{LL'} + \sum_{n'',L''} g^{nn''}_{LL''}\, t^{n''}_{l''}\, g^{n''n'}_{L''L'} + \sum_{n'',L''}\sum_{n''',L'''} g^{nn''}_{LL''}\, t^{n''}_{l''}\, g^{n''n'''}_{L''L'''}\, t^{n'''}_{l'''}\, g^{n'''n'}_{L'''L'} + \cdots \,, \tag{95}$$

meaning that an the electron can travel from n' to n directly, or after being scattered once by any site, or by two sites, etc.

In practice, the structural Green functions are first calculated in $\vec{k}$-space using matrix inversion; a subsequent Fourier transform gives us the real-space quantities. We write, then,

$$G_{LL'}(\vec{k};E) = \sum_{n'} G_{LL'}^{nn'}(E)\, e^{-i\vec{k}\cdot(\vec{R}^n-\vec{R}^{n'})} \tag{96}$$

(which, due to translational symmetry, is independent of n). The algebraic Dyson equation (94) becomes

$$G_{LL'}(\vec{k};E) = g_{LL'}(\vec{k};E) + \sum_{L''} g_{LL''}(\vec{k};E)\, t_{l''}(E)\, G_{L''L'}(\vec{k};E) \tag{97}$$

(the t-matrix is independent of n, again due to translational symmetry). The structural Green functions $G_{LL'}$ and $g_{LL'}$, and the t-matrix t_l, are considered as matrices in L and L', and (97) is solved by matrix inversion after a cutoff at some $l = l_{\max}$ for which the t-matrix becomes negligible (usually $l_{\max} = 3$ or 4 suffices). The result is

$$G_{LL'}^{nn'}(E) = \frac{1}{V_{\mathrm{BZ}}} \int_{\mathrm{BZ}} d^3k\, e^{i\vec{k}\cdot(\vec{R}^n-\vec{R}^{n'})} \left[\Big(1 - \mathbf{g}(\vec{k};E)\,\mathbf{t}(E)\Big)^{-1} \mathbf{g}(\vec{k};E)\right]_{LL'} \tag{98}$$

where the integral is over the Brillouin zone volume V_{BZ}. For the calculation of the charge density or of the density of states, only the on-site term $n = n'$, $G_{LL'}^{nn}(E)$, is needed.

It is straightforward to generalize the method to the case of more than one atoms per unit cell, say N_{at}. Introducing an index $\mu = 1, \ldots, N_{\mathrm{at}}$ to account for the different atom types, and reserving the index n for the periodic lattice positions, an atomic position in the crystal is defined by the lattice vector $\vec{R}^n$ plus the site vector $\vec{\chi}^\mu$ connecting the lattice point to the basis atom:

$$\vec{R}^{n\mu} = \vec{R}^n + \vec{\chi}^\mu. \tag{99}$$

The Fourier transforms are done then with respect to n only, so that we have an expression analogous to Eq. (96),

$$G_{LL'}^{\mu\mu'}(\vec{k};E) = \sum_{n'} G_{LL'}^{n\mu,n'\mu'}(E)\, e^{-i\vec{k}\cdot(\vec{R}^n-\vec{R}^{n'})}, \tag{100}$$

and the analogous Fourier transform for the free-space structure constants $g^{n\mu,n'\mu'}$, giving the amplitude of electron propagation from atom μ' at lattice position n' to atom μ at lattice position n. The Dyson equation (98) then takes the form

$$\begin{aligned} G_{LL'}^{n\mu,n'\mu'}(E) = \frac{1}{V_{\mathrm{BZ}}} \int_{\mathrm{BZ}} & d^3k\, e^{i\vec{k}\cdot(\vec{R}^n-\vec{R}^{n'})}\, e^{i\vec{k}\cdot(\vec{\chi}^\mu-\vec{\chi}^{\mu'})} \\ & \times \left[\Big(1 - \mathbf{g}(\vec{k};E)\,\mathbf{t}(E)\Big)^{-1} \mathbf{g}(\vec{k};E)\right]_{LL'}^{\mu\mu'}. \end{aligned} \tag{101}$$

Here, the t-matrix $\mathbf{t}(E)$ depends on the atom-type μ and on angular-momentum indexes (it is site-diagonal, $(\mathbf{t})_l^{\mu\mu'} = t_l^\mu\, \delta_{\mu\mu'}$). The structure constants $\mathbf{g}(\vec{k};E)$ are considered as matrices in both (L, L') and (μ, μ'), and thus the computational effort for the matrix inversion increases as $O(N_{\mathrm{at}}^3)$. A considerable speed-up can be achieved for large systems by using the concept of the screening transformation (see Section 8).

6 Description of the Full-Potential

Although the approximation of spherical potentials around the atomic gives in many cases reasonable results, the correct description of the full anisotropic potential can give significant corrections when details of the electronic structure are required. The full-potential can be especially important in systems of reduced symmetry, such as non-cubic crystals, at surfaces or interfaces, etc.; in particular the calculation of forces on atoms, leading to lattice relaxations, is highly inaccurate without the full-potential. In this section we give a summary of the full-potential treatment within the KKR method, and refer to the literature for details, concerning in particular the convergence properties.[27]

We begin our discussion on the level of scattering theory by a single anisotropic potential $V(\vec{r})$ of finite maximal radius S, which later will represent the site-centered atomic potential of a crystal. An incoming wave of wavevector $\vec{k}$, scattered by this potential, results in a wave $\psi_{\vec{k}}(\vec{r})$. The dependence on $\vec{k}$ is lifted by an expansion in spherical harmonics:

$$\psi_{\vec{k}}(\vec{r}) = \sum_{L'} 4\pi i^{l'} Y_{L'}(\vec{k}) R_{L'}(\vec{r};E), \tag{102}$$

where $R_{L'}(\vec{r};E)$ is the regular (converging at zero) solution of the Schrödinger equation corresponding to an incoming spherical wave of symmetry L'. The Lippmann-Schwinger equation, determining $R_{L'}(\vec{r};E)$, is

$$R_{L'}(\vec{r}) = j_{l'}(\sqrt{E}r) Y_{L'}(\vec{r}) + \int g(\vec{r},\vec{r}\,';E) V(\vec{r}\,') R_{L'}(\vec{r}\,')\, d^3r', \tag{103}$$

where the incoming free wave $j_{l'}(\sqrt{E}r)Y_L(\vec{r})$ and the free-electron Green function $g(\vec{r},\vec{r}\,';E)$ appear. While the index L' refers to the incoming wave, the wavefunction $R_{L'}(\vec{r}\,')$ can be expanded once more[28] in spherical harmonics to lift the dependence on the direction of $\vec{r}$ (if the potential is spherically symmetric, $R_{L'}(\vec{r})$ is just $R_{l'}(r)Y_{L'}(\vec{r})$):

$$R_{L'}(\vec{r}) = \sum_L R_{LL'}(r;E)\, Y_L(\vec{r}). \tag{104}$$

Similarly, the potential $V(\vec{r})$ is expanded in spherical harmonics as

$$V(\vec{r}) = \sum_L V_L(r) Y_L(\vec{r}). \tag{105}$$

Using these expansions, the Lippmann-Schwinger equation (103) can be re-written in the form

$$R_{LL'}(r;E) = j_l(\sqrt{E}r)\, \delta_{LL'} + \int_0^S g_l(r,r';E) \sum_{L''} V_{LL''}(r') R_{L''L'}(r';E)\, r'^2\, dr' \tag{106}$$

where we have introduced the notation

$$V_{LL'}(r) = \sum_{L''} C_{LL'L''} V_{L''}(r). \tag{107}$$

The advantage of Eq. (106) is that it contains only a one-dimensional integral instead of the three-dimensional integral of (103). However, one has now to solve a system of coupled radial equations, since the Schrödinger equation reads:

$$\sum_{L''}\left[\left(-\frac{1}{r}\frac{\partial^2}{\partial r^2}r+\frac{l(l+1)}{r^2}-E\right)\delta_{LL''}+V_{LL''}\right]R_{L''L'}(r;E)=0\ . \tag{108}$$

Obviously, the non-spherical components of the potential mix the angular-momentum channels, resulting in the above coupled equations. Also the t-matrix contains now mixed angular-momentum components. It is found by matching $R_{L''L'}$ to an outgoing free wave at the boundary S, and related to the solution $R_{L''L'}$ by:

$$t_{LL'}(E)=\int_0^S j_l(\sqrt{E}r)\sum_{L''}V_{LL''}R_{L''L'}(r';E)\,r'^2\,dr' \tag{109}$$

which is analogous to expression in Eq. (61) for the spherical potential. Similar to $R_L(\vec{r};E)$, the irregular (diverging at the origin) solution of the Schrödinger equation, $H_L(\vec{r};E)$, is expanded in spherical harmonics as

$$H_{L'}(\vec{r};E)=\sum_L H_{LL'}(r;E)Y_L(\vec{r}). \tag{110}$$

Instead of solving directly the coupled Schrödinger equations, a different procedure is followed, based on perturbation theory. Since the non-spherical part of the potential is usually weak compared to the spherical part, first the radial solutions $R_l^{\mathrm{sph}}(r;E)$ and $H_l^{\mathrm{sph}}(r;E)$ for the spherical component ($V_{l=0}(r)$) are calculated, as in Section 3 (see Eq. (53)). This is used as a reference system. Then, using also the corresponding spherical Green function

$$G_l^{\mathrm{sph}}(r,r';E)=-i\sqrt{E}R_l^{\mathrm{sph}}(r<;E)H_l^{\mathrm{sph}}(r>;E) \tag{111}$$

(see also eq. (68)), the radial wavefunctions of the non-spherical case are connected to $R_l^{\mathrm{sph}}(r;E)$ via the Lippmann-Schwinger equation

$$R_{LL'}(r;E)=R_l^{\mathrm{sph}}(r;E)\delta_{LL'}+\int_0^S G_l^{\mathrm{sph}}(r,r';E)\sum_{L''}\Delta v_{LL''}(r')R_{L''L'}(r';E)r'^2\,dr' \tag{112}$$

where only the non-spherical part of the potential enters:

$$\Delta v_{LL'}(r)=\sum_{L''\neq 0}C_{LL'L''}V_{L''}(r). \tag{113}$$

Eq. (112) can be solved iteratively, as a Born series. Practice shows that two or three iterations are enough for most applications. Similar is the solution for the irregular wavefunction $H_{LL'}(\vec{r};E)$, starting from $H_l^{\mathrm{sph}}(r>;E)$.

Within a crystal, the site-centered potentials must be cut off at the boundary of the Wigner-Seitz cells. In order to ensure this, shape functions are used[29] and expanded in spherical harmonics. In particular, the shape function $\Theta^n(\vec{r})$ of a site n is defined as

$$\Theta^n(\vec{r})=\begin{cases}1 \text{ if } \vec{r} \text{ is in the WS-cell of site } n,\\ 0 \text{ otherwise.}\end{cases} \tag{114}$$

The crystal potential is then given by

$$V^n(\vec{r})=V(\vec{r}+\vec{R}^n)\,\Theta^n(\vec{r}). \tag{115}$$

The shape functions are expanded as

$$\Theta^n(\vec{r}) = \sum_L \Theta_L^n(r) Y_L(\vec{r}). \tag{116}$$

The coefficients $\Theta_L^n(r)$ enter in the expansions for the charge density and the potential, in order to ensure the correct cutoff at the Wigner-Seitz boundary. Without going into details, we note that, although the convergence of Eq. (116) is slow, the property of the Gaunt coefficients

$$C_{LL'L''} \neq 0 \;\text{ only if } |l' - l''| \leq l \leq l' + l'' \tag{117}$$

allows us to take into account the shape functions up to only $4l_{\mathrm{max}}$, if the t-matrix and the Green functions are cut off at l_{max}.

7 Total Energy

Within density functional theory, the total energy of a many-electron system is written as a sum of three terms: the single-particle kinetic energy $T[\rho_s]$, the Hartree energy $E_H[\rho]$, and the exchange and correlation energy $E_{xc}[\rho_s]$ ($s = (+,-)$ is the spin index). The kinetic and the exchange-correlation energy, as well as the total energy, are functionals of the spin density $\rho_s(\vec{r}) := (\rho_+(\vec{r}), \rho_-(\vec{r}))$, while the Hartree energy is a functional of the charge density $\rho = \rho_+ + \rho_-$. We have:

$$E_{\mathrm{tot}}[\rho_+, \rho_-] = T[\rho_+, \rho_-] + E_H[\rho] + E_{xc}[\rho_+, \rho_-] \; . \tag{118}$$

Given the single-particle energies ϵ_{is} (eigenenergies of the Kohn-Sham equations), the kinetic energy can be written in terms of these and of the effective Kohn-Sham potential $V_s^{\mathrm{eff}}(\vec{r})$ as:

$$T[\rho_+, \rho_-] = \sum_s \left(\sum_i \epsilon_{is} - \int \rho_s(\vec{r})\, V_s^{\mathrm{eff}}(\vec{r})\, d^3r \right) \; . \tag{119}$$

In this way, the sum of the single-particle energies

$$E_{\mathrm{SP}} := \sum_{is} \epsilon_{is} \tag{120}$$

is singled out and can be thought of a "band energy", which would be relevant if we had non-interacting electrons in an external potential, while the remaining terms are packed up together in what is called the "double-counting energy terms", as corrections to the single-particle picture:

$$E_{\mathrm{DC}}[\rho_+, \rho_-] = -\sum_s \int \rho_s(\vec{r})\, V_s^{\mathrm{eff}}(\vec{r})\, d^3r + E_H[\rho] + E_{xc}[\rho_+, \rho_-]. \tag{121}$$

The total energy is the sum of the two:

$$E_{\mathrm{tot}}[\rho_+, \rho_-] = E_{\mathrm{SP}}[\rho_+, \rho_-] + E_{\mathrm{DC}}[\rho_+, \rho_-]. \tag{122}$$

We proceed to analyze each term separately. The sum of single-particle energies can be written in terms of the spin-dependent density of states $n_s(E)$ as

$$E_{\rm SP} = \sum_{is} \epsilon_{is}$$

$$= \sum_s \int^{E_F} E\, n_s(E)\, dE \tag{123}$$

$$= E_F N - \sum_s \int^{E_F} N_s(E)\, dE. \tag{124}$$

In the last step we introduced $N_s(E)$ as the integrated density of states up to energy E and used the fact that the total number of electrons per spin is just $N_s = \int_{E_F} n(E)\, dE$, and $N = N_+ + N_-$. In practice, expression in Eq. (123) can be used for periodic systems. Expression in Eq. (124) is useful for systems with broken periodicity, such as impurities in crystals, where the perturbed charge density converges very slowly with distance from the impurity due to Friedel oscillations. Then, $N_s(E)$ is calculated not by integration of $n_s(E)$, but by using the Friedel sum rule (or its multiple-scattering analogue, Lloyd's formula), which takes into account the Friedel oscillations up to infinity.

The double-counting term includes the electrostatic energy and the exchange-correlation energy. The electrostatic (Hartree) energy depends on the charge densities at each cell n, $\rho_n(\vec{r}) := \rho(\vec{r} + \vec{R}^n)$, and on the nuclear charges Z^n. We have:

$$E_H[\rho] = \sum_{nn'} \int_{\Omega^n} d^3r \int_{\Omega^{n'}} d^3r' \frac{\rho^n(\vec{r})\, \rho^{n'}(\vec{r}\,')}{|\vec{r} + \vec{R}^n - \vec{r}\,' - \vec{R}^{n'}|}$$

$$-2 \sum_{nn'} Z^{n'} \int_{\Omega^n} d^3r \frac{\rho^n(\vec{r})}{|\vec{r} + \vec{R}^n - \vec{R}^{n'}|} + \sum_n \sum_{n' \neq n} \frac{Z^n Z^{n'}}{|\vec{R}^n - \vec{R}^{n'}|} \tag{125}$$

where Ω^n is the volume of the atomic cell n. It proves convenient to define the Coulomb potential

$$V_C^n(\vec{r}) = 2 \sum_{n'} \int_{\Omega^{n'}} d^3r' \frac{\rho^{n'}(\vec{r}\,')}{|\vec{r} + \vec{R}^n - \vec{r}\,' - \vec{R}^{n'}|} - 2 \sum_{n'} \frac{Z^{n'}}{|\vec{R}^n - \vec{R}^{n'}|}\ . \tag{126}$$

The Madelung potential $V_M(\vec{R}^n)$ is the Coulomb potential at position R^n if we exclude the term $n' = n$ from the second sum of (126):

$$V_M(\vec{R}^n) = 2 \sum_{n'} \int_{\Omega^{n'}} d^3r' \frac{\rho^{n'}(\vec{r}\,')}{|\vec{r} + \vec{R}^n - \vec{r}\,' - \vec{R}^{n'}|} - 2 \sum_{n'(\neq n)} \frac{Z^{n'}}{|\vec{R}^n - \vec{R}^{n'}|}\ . \tag{127}$$

Using the above definitions we re-write the electrostatic energy as

$$E_H[\rho] = \frac{1}{2} \left[\sum_n \int_{\Omega^n} d^3r\, \rho^n(\vec{r}) V_C^n(\vec{r}) - \sum_n Z^n V_M(\vec{R}^n) \right]\ . \tag{128}$$

The Coulomb potential and the charge density at site n are expanded in spherical harmonics around $\vec{R}^n$:

$$V_C^n(\vec{r}) = \sum_L V_{C,L}^n(r) Y_L(\vec{r}); \tag{129}$$

$$\rho^n(\vec{r}) = \sum_L \rho_L^n(r) Y_L(\vec{r}). \tag{130}$$

In this way the calculation of the Coulomb potential is reduced to summing up terms containing the moments $\rho_L^n(r)$ of the charge density over all lattice sites. For the higher l terms the corresponding summations converge rapidly, but for low l an Ewald summation is required. The details of this procedure are omitted here. Once the expansion in Eq. (129) of the Coulomb potential is known, the Madelung potential can be calculated using the value of V_C^n at a sphere of radius R around $\vec{R}^n$ and by knowledge of the charge distribution within this sphere. The result can be obtained by solving the corresponding boundary-value problem in electrostatics (the proof is omitted here):

$$V_M(\vec{R}^n) = 2\sqrt{4\pi} \int_0^R \rho_{l=0}^n(r)\, dr + \frac{2}{R}(Z^n - N^n(R)) + \frac{1}{\sqrt{4\pi}} V_{C,l=0}^n(R), \tag{131}$$

where $N^n(R)$ is the number of electrons within the sphere of radius R.

The effective Kohn-Sham potential at cell n can be written in terms of the Coulomb potential and the exchange-correlation energy:

$$V_{\text{eff}\, s}^n(\vec{r}) = V_C^n(\vec{r}) + \frac{\delta E_{xc}[\rho_+, \rho_-]}{\delta \rho_s(\vec{r})}. \tag{132}$$

Finally, the exchange-correlation energy within the local density approximation is given by

$$E_{xc}^{\text{LDA}}[\rho] = \int \rho(\vec{r})\, \epsilon_{xc}(\rho_+(\vec{r}), \rho_-(\vec{r}))\, d^3r \tag{133}$$

where $\epsilon_{xc}(\rho+, \rho_-)$ is the exchange-correlation energy density for a homogeneous electron gas of spin density ρ_s. This is again expanded in spherical harmonics as

$$\epsilon_{xc}(\rho_+^n(\vec{r}), \rho_-^n(\vec{r})) = \sum_L \epsilon_{xc,L}^n(r) Y_L(\vec{r}), \tag{134}$$

and the exchange-correlation energy is given by

$$E_{xc}^{\text{LDA}}[\rho] = \sum_n \sum_{LL'L''} C_{LL'L''} \int_0^{R_c^n} \Theta_L^n(r)\, \rho_{L'}^n(r)\, \epsilon_{xc,L''}^n(r)\, r^2\, dr. \tag{135}$$

8 Screened (Tight-Binding) KKR Method

An improvement of the KKR method has been achieved by the so-called *screened* or *tight-binding* KKR formalism,[8] which allows a considerable reduction of the calculation time for large systems. In particular, while the traditional KKR formalism requires a matrix inversion for the solution of the algebraic Dyson equation with computational effort of $O(N^3)$ (for N different atoms in the unit cell), in the screened KKR method the same results can be obtained with an effort of, ideally, $O(N)$; this is optimally achieved for layered systems. This is made possible by a transformation of the reference system after which the reference Green function falls off exponentially with distance, thus allowing the inversion of sparse, or even tridiagonal, matrices, which is much faster than a full matrix inversion. Due to the decoupling between distant atomic sites which follows, the corresponding transformation is called *screening transformation* and the method *screened KKR*; due to its formal resemblance to tight-binding theory, the method is also called *tight-binding KKR*.

Three observations lead to the tight-binding KKR formalism:

- Using the Dyson equation one can connect the crystal Green function to any reference system (of the same periodic structure), and not just to the free electron system.
- A reference system of repulsive potentials can be constructed in which there are no states in the energy region of interest (up to 1-2 Ry higher than E_F).
- The structural Green functions of this reference system fall off exponentially in space, so that the corresponding KKR matrix becomes practically sparse or tridiagonal.

In what follows, we shall describe these ideas in more detail.

8.1 Transformation to an Arbitrary Reference System

In the Dyson equation, introduced in Section 2, no formal statement is made about the nature of the reference system. Subsequently, when describing the KKR method, we have chosen a reference system of constant potential as the most natural one, since the Green function and structure constants are then given by simple analytical expressions. Here we show that a choice of another reference system of the same lattice structure as the real system leads to the same form of the algebraic Dyson equation, with the difference of t-matrices between the real and reference system ($t^n_{LL'}(E) - t^{r,n}_{LL'}(E)$) entering in the place of the $t^n{}_{LL'}(E)$ in Eq. (94).

Consider then a reference system of potentials $V^{r,n}(\vec{r})$ (to be given in detail below) placed at the lattice sites n of the crystal. These are characterized by t-matrices $t^{r,n}(E)$. The structural Green function of this system, $G^{r,nn'}_{LL'}(E)$, are related to the free-space structure constants, $g^{nn'}_{LL'}(E)$ (Eq. (72)), via the algebraic Dyson equation. Adopting boldface symbols to denote matrices (and with $\mathbf{t}^r$ standing for the site-diagonal t-matrix), this is written

$$\mathbf{G}^r(E) = \mathbf{g}(E) + \mathbf{g}(E)\,\mathbf{t}^r(E)\,\mathbf{G}^r(E) \tag{136}$$

which is rewritten as

$$(\mathbf{G}^r)^{-1} = \mathbf{g}^{-1} - \mathbf{t}^r. \tag{137}$$

At the same time the structural Green functions of the real system, $G^{nn'}_{LL'}(E)$, are related to the free-space structure constants via the t-matrix $t^n(E)$ of the real system. The corresponding algebraic Dyson equation reads:

$$(\mathbf{G})^{-1} = \mathbf{g}^{-1} - \mathbf{t}. \tag{138}$$

Expressions in Eqs. (136) and (137) lead directly to the algebraic Dyson equation connecting the new reference system to the real system:

$$(\mathbf{G})^{-1} = (\mathbf{G}^r)^{-1} - (\mathbf{t} - \mathbf{t}^r), \tag{139}$$

which can be expanded as

$$\mathbf{G}(E) = \mathbf{G}^r(E) + \mathbf{G}^r(E)\,\Delta\mathbf{t}(E)\,\mathbf{G}(E) \tag{140}$$

with $\Delta\mathbf{t}(E) = \mathbf{t}(E) - \mathbf{t}^r(E)$. This equation has the same form as Eq. (94) with $\Delta\mathbf{t}(E)$ in the place of $\mathbf{t}(E)$.

8.2 Choice of a Reference System of Repulsive Potentials

Having shown that the algebraic Dyson equation holds after a transformation to a new reference system, we proceed with the choice of an adequate reference system in which the structural Green functions fall exponentially with distance. Such a system is defined by a collection of repulsive muffin-tin potentials (one around each site n) of the form:

$$V^{r,n}(\vec{r}) = \begin{cases} V_{\mathrm{C}},\ r \leq R^n_{\mathrm{MT}} \\ 0, \quad \text{otherwise} \end{cases} \tag{141}$$

with R^n_{MT} the muffin-tin radius at site n, and V_{C} a positive constant, usually chosen to be a few Rydbergs. It is physically expected (and computationally verified) that for such a potential the eigenvalue spectrum starts from an energy E_{bot} somewhat smaller that V_{C}; a choice of $V_{\mathrm{C}} = 4$ Ry is adequate to push E_{bot} high above E_F. Schematically, this is shown in Figure 1.

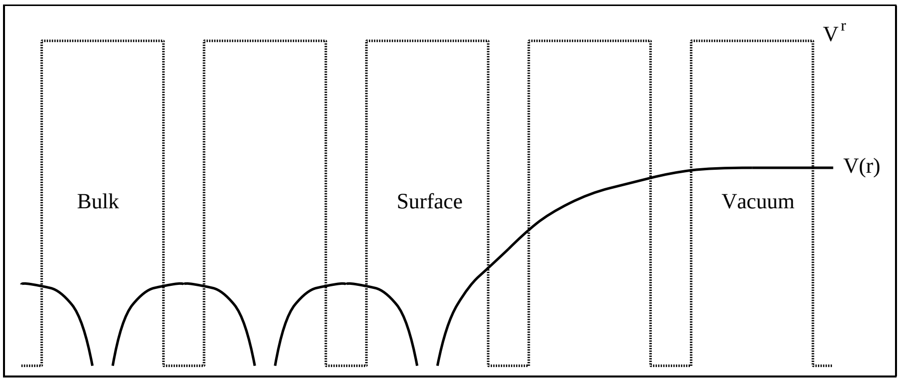

Figure 1. Schematic representation of the repulsive potential $V^r(\vec{r})$ and the crystal potential $V(\vec{r})$ in the bulk, at a surface, and in the vacuum.

In this way, it is ensured that for $E < E_{\mathrm{bot}}$ the Green function of the reference system drops rapidly, and in practice exponentially, with distance; the same is true for the structural Green functions. In order to demonstrate this, we introduce the *partial norm*

$$N_{ll'}(|\vec{R}n - \vec{R}^{n'}|; E) = \frac{|E|^{(l+l')/2}}{(2l+1)!!(2l'+1)!!} \left[\sum_{mm'} |G^{r,nn'}_{lm,l'm'}(E)|^2 \right]^{1/2} \tag{142}$$

with $(2l+1)!! = (2l+1)(2l-1)\dots(3)(1)$. In Figure 2 (left), the partial norms for an fcc lattice are plotted for $l = l'$ as function of the distance $|\mathbf{R}^{nn'}|$ for the choice $E = 0.65$ Ry which is representative for the Fermi energy of Cu. They are compared with the corresponding norms of the Green function g for potential-free space in Figure 2 (right panel).[8]

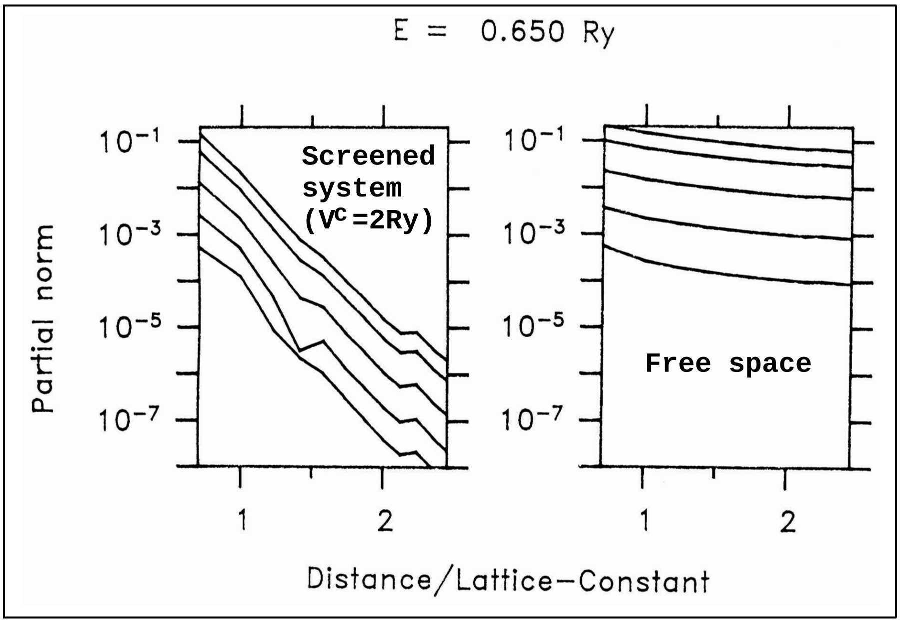

Figure 2. Screened (left panel) and unscreened (right panel) partial norms (Eq. (142)) for $l = l'$ and $E = 0.65$ Ry as function of the distance in units of the lattice constant for an fcc lattice. The results for $l = 0, 1, 2, 3, 4$ are shown from top to bottom.[8]

The rapid decay of these *screened* structural Green functions allows their direct evaluation in real space, with no need of a Brillouin zone integration. Thus the cumbersome calculation of the free-space $g_{LL'}(\vec{k}; E)$, which demands an Ewald summation for convergence, is avoided. Instead, the matrices in equation (136) can be cut off in real space at a finite value of $|\vec{R}^n - \vec{R}^{n'}|$ (two lattice constants are enough for fcc), and solved by direct matrix inversion, yielding $G^{r,nn'}_{LL'}(E)$; it is straightforward to obtain $G^r_{LL'}(\vec{k}; E)$ by a subsequent Fourier transform, since the summand is confined to finite $|\vec{R}^n - \vec{R}^{n'}|$.

8.3 Calculational Speed-up for Large Systems

At the end of Section 5 we commented that the computational effort for large systems, with many atoms per unit cell, scales as $O(N_{\mathrm{at}}^3)$ due to the matrix inversion involved in the Dyson equation (see Eq. (101)). We will now see why the screening transformation allows for a considerable acceleration of the calculations.

Using the notation introduced at equations (99–101), we consider the Fourier-transformed structural Green functions of a large system, and the algebraic Dyson equation after the screening transformation:

$$G^{\mu\mu'}_{LL'}(\vec{k};E) = \left[\left(1 - \mathbf{G}^r(\vec{k};E)\,\Delta\mathbf{t}(E)\right)^{-1}\mathbf{G}^r(\vec{k};E)\right]^{\mu\mu'}_{LL'}. \tag{143}$$

For large systems, where the interatomic distance in the unit cell is large for several pairs of atoms, the reference structural Green functions $|\mathbf{G}^{r,\mu\mu'}|$ are practically vanishing for the corresponding (μ,μ') and can be neglected. Then the matrix which must be inverted in Eq. (143) is sparse, and one can use algorithms for inversion and multiplication of sparse matrices to speed up the calculation. Moreover, one matrix multiplication in (143) can be avoided by converting the equation as:

$$\mathbf{G} = (1 - \mathbf{G}^r\,\Delta\mathbf{t})^{-1}\mathbf{G}^r = -\Delta\mathbf{t}^{-1} + \Delta\mathbf{t}^{-1}\left(\Delta\mathbf{t}^{-1} - \mathbf{G}^r\right)^{-1}\Delta\mathbf{t}^{-1}. \tag{144}$$

Since the t-matrix is site-diagonal, the inversion $\mathbf{t}^{-1}$ and the multiplications with $\mathbf{t}^{-1}$ are numerically inexpensive.

This is particularly important in the case of layered systems, which are extending over many monolayers in one direction. Then the indexes μ,μ' are layer indexes, and reference structural Green function matrix takes a block-tridiagonal form, given schematically as

$$\begin{bmatrix} x\ x\ 0\ 0\ \ldots\ 0\ 0\ 0\ x \\ x\ x\ x\ 0\ \ldots\ 0\ 0\ 0\ 0 \\ 0\ x\ x\ x\ \ldots\ 0\ 0\ 0\ 0 \\ 0\ 0\ x\ x\ \ldots\ 0\ 0\ 0\ 0 \\ \ldots\ldots\ldots\ldots\ldots\ldots \\ 0\ 0\ 0\ 0\ \ldots\ x\ x\ 0\ 0 \\ 0\ 0\ 0\ 0\ \ldots\ x\ x\ x\ 0 \\ 0\ 0\ 0\ 0\ \ldots\ 0\ x\ x\ x \\ x\ 0\ 0\ 0\ \ldots\ 0\ 0\ x\ x \end{bmatrix}. \tag{145}$$

Each symbol x represents a matrix block, with its size being related to the distance $|\vec{\chi}^{\mu} - \vec{\chi}^{\mu'}|$ after which $|G^{r,\mu\mu'}_{LL'}|$ is considered negligible; the x at the upper right and lower left corners are present only if we have a repeated supercell. If only first neighbors would couple, the blocks would be matrices in L and L' only (of size $(l_{\max}+1)^2 \times (l_{\max}+1)^2$). For longer-range coupling one can use the principal layer technique by which several layers are combined into a principal layer such that only nearest neighboring principal layers couple. Then one obtains again the form Eq. (144), but now the blocks are submatrices with L and L' indexes and i and i' indexes enumerating the layers within the principal layer. The matrix structure displayed in Eq. (144) is the appropriate one for the multilayer geometry, whereas in slab geometry the lowest left block and the highest right block vanish. For surfaces and interfaces of half-infinite crystals the matrix (Eq. (144)) has infinite range to one or both sides.

In any case the numerical complexity is greatly reduced from $O(N^3)$ to $O(N)$ for N different and $O(\log N)$ for N identical principal layers. Note that, for the calculation of the spin density (and therefore for self-consistent calculations), only the on-site terms of the real-system structural Green function are needed,[e] i.e., the block-diagonal part ($\mu' = \mu$)

[e] Because $\rho_s(\vec{R}^{\mu}+\vec{r}) = -\frac{1}{\pi}\mathrm{Im}\int_{-\infty}^{E_F} G_s(\vec{R}^{\mu}+\vec{r},\vec{R}^{\mu}+\vec{r};E)\,dE$.

of $G^{\mu\mu'}_{LL'}$. This fact is included in the $O(N)$ speed-up; if one wishes to calculate additional, non-diagonal matrix elements of $G^{\mu\mu'}_{LL'}$, e.g. for impurity or transport calculations, the numerical cost is $O(N)$ for each additional element, giving a total of $O(N^3)$ if all N^2 elements are to be calculated.

The treatment of matrices like Eq. (144) is well known in tight-binding surface physics and, for instance for the tight-binding linear-muffin-tin-orbital method,[30] Wenzien et al.[31] have presented an efficient formalism to calculate the Green function of an ideal semi-infinite crystal and the corresponding $\mathbf{k}_{\|}$ resolved densities of states.

9 Two-Dimensional Systems: Finite-Thickness Slabs and Half-Infinite Crystals

The extension of the KKR method to the treatment of layered systems, such as surfaces and interfaces, is straightforward, and most efficient within the screened KKR formalism, where $O(N)$ scaling can be achieved (where N is the number of layers) as discussed in Section 8.

When treating a layered system, a surface-adapted geometry is used, in the sense that the two-dimensional periodicity of the atomic layers parallel to the surface (or interface) is exploited while the direction perpendicular to these layers is treated as if these were different atoms in a unit cell. The Fourier transforms are done now within the two-dimensional surface Brillouin zone (SBZ), and the corresponding integration is over all $\vec{k}_{\|}$ in the SBZ. Thus, we have the analogue of Eq. (101),

$$G^{n\mu,n'\mu'}_{LL'}(E) = \frac{1}{A_{\rm SBZ}} \int_{\rm SBZ} d^2k_{\|}\, e^{i\vec{k}_{\|}\cdot(\vec{R}^n - \vec{R}^{n'})}\, e^{i\vec{k}_{\|}\cdot(\vec{\chi}^\mu - \vec{\chi}^{\mu'})} \times \left[\Big(1 - \mathbf{G}^r(\vec{k}_{\|};E)\,\Delta\mathbf{t}(E)\Big)^{-1} \mathbf{G}^r(\vec{k}_{\|};E)\right]^{\mu\mu'}_{LL'}. \qquad (146)$$

where now $\vec{R}^n$ are in-plane position vectors of the two-dimensional Bravais lattice, while $\vec{\chi}^\mu$ are vectors connecting atomic positions in different layers; $A_{\rm SBZ}$ is the area of the SBZ.

In the case of surfaces, the vacuum is described by empty sites, meaning that the lattice structure is continued into the vacuum but no nuclei are positioned there. In this way, the vacuum potential and charge density are calculated within the multiple-scattering formalism on the same footing as the bulk. In practice, three or four monolayers of vacuum sites are enough for the calculation of the electronic structure; Eq. (146) can be cutoff after that.

Depending on the problem, one can choose to use a slab of finite thickness in order to represent a surface or interface, or one can choose to take half-infinite boundary conditions. In the latter case, and starting from a "boundary" layer, the crystal is continued by periodically repeating the potential of this boundary layer to all subsequent layers up to infinity. One is then faced with a problem of inverting an infinite matrix, which due to the screening transformation has a tridiagonal form (see expression (145)), in order to find the Green function in the region of interest. This is done efficiently by the decimation technique,[32] which is based on an iterative inversion of matrices of doubled size at each step. In this way the number of layers which are included in the Green function grows exponentially with the number of steps, and the limit of the half-infinite crystal is rapidly achieved.

10 Self-Consistency Algorithm and Energy Contour Integration

We proceed with a short description of the self-consistency algorithm for the calculation of the electronic structure by the KKR method. As in all first-principles schemes, the central quantity is the charge density which is found by solving the Kohn-Sham equations. The steps followed are:

1. Start with an input potential V_s^{in} (s is a spin index used in magnetic systems).
2. Calculate the wavefunctions R_L and H_L and, from these, the t-matrix $t_{LL'}$.
3. Calculate the structure constants of the reference system $g_{LL'}^{\mathrm{ref}}(\vec{k};E)$ (or the free-space structure constants if the tight-binding formalism is not used).
4. Calculate the t-matrix of the reference system, $t_{LL'}^{\mathrm{ref}}$, and the difference $\Delta t_{LL'} = t_{LL'} - t_{LL'}^{\mathrm{ref}}$.
5. Solve the algebraic Dyson equation by matrix inversion for the structural Green function and integrate over $\vec{k}$ (see Eq. (98) for $n = n'$ and for Δt in the place of t).
6. Calculate the Green function using the structural Green function and R_L and H_L (Eq. (92)). Integrate the Green function from the bottom of the valence band E_b up to E_F using a complex-energy contour (see below) and take the imaginary part to find the valence electron spin density: $\rho_s^v(\vec{r}) = -\frac{1}{\pi}\mathrm{Im}\int_{E_b}^{E_F} G_s(\vec{r},\vec{r};E)\,dE$.
7. Calculate the core-electron wavefunctions and core-electron spin density $\rho_s^c(\vec{r})$; here the multiple-scattering formalism is not needed, because the core wavefunctions are assumed to be highly localized at the atomic sites. Obtain the total spin density $\rho_s = \rho_s^c + \rho_s^v$.
8. Find the output potential V_s^{out} by solving the Poisson equation and adding the exchange-correlation potential. If $V_s^{\mathrm{out}} = V_s^{\mathrm{in}}$ to a reasonable accuracy, exit the cycle, otherwise:
9. Properly mix V_s^{out} with V_s^{in} to obtain a new input potential, and return to step 1.

We now comment on the energy integration for the valence charge density or spin density. According to Eq. (21), the integral to be taken is

$$\rho_s^v(\vec{r}) = -\frac{1}{\pi}\mathrm{Im}\int_{E_b}^{E_F} G_s(\vec{r},\vec{r};E)\,dE\ . \tag{147}$$

In order to reach the desired accuracy for achieving self-consistency, a large number of integration points are required for the evaluation of Eq. (147), typically between 1000 and 2000. Fortunately, the numerical effort can be strongly reduced by using the analytical properties of the Green function. Since $G(E)$ is analytical on the upper energy half-plane ($\mathrm{Im}E > 0$), the integral in Eq. (147) can be evaluated on a contour starting at the real axis below E_b, continuing at complex $E = E_R + i\Gamma$ (with $E_R = \mathrm{Re}E$), and ending at E_F.[33] The gain comes from the fact that, for larger Γ, the Green function has much less structure than at the real axis. This can be understood by considering that the density of states corresponding to an eigenvalue ϵ_i is of the form $-\frac{1}{\pi}\mathrm{Im}G(E) = \delta(E-\epsilon_i)$ for real E, while it takes the form $-\frac{1}{\pi}\mathrm{Im}G(E_R+i\Gamma) = \Gamma\pi^{-1}/((E_R-\epsilon_i)^2+\Gamma^2)$ for complex E, i.e., it is broadened to a Lorentzian function of half-width Γ. As a result, 30 integration points are typically enough when integrating over such a contour. Furthermore, for the energies far from the real axis, fewer k-points are needed in the Brillouin zone integration (Eq. (98)), reducing even more the numerical cost.

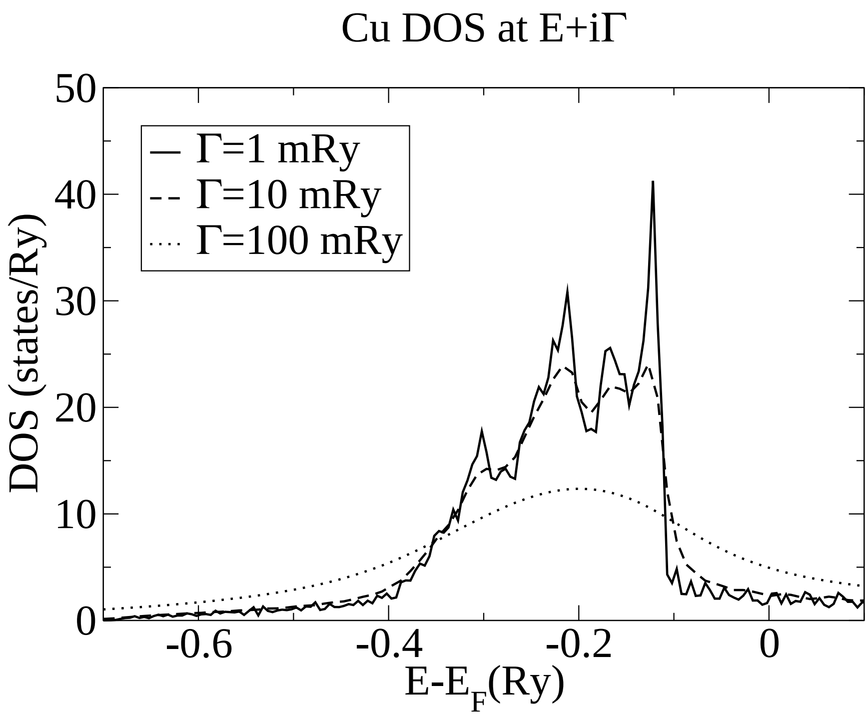

Figure 3. Density of states (DOS) of fcc Cu calculated for $\Gamma = 100$ mRy (typical for self-consistency calculations), 10 mRy, and 1 mRy (typical for density-of-states calculations). The smoothening of the Green function for larger Γ, leading to a drastic decrease of the number of necessary integration points, is evident.

In order to demonstrate the smoothening of the Green function with increasing Γ, we show in Figure 3 the density of states of fcc Cu calculated for $\Gamma = 100$ mRy (typical for self-consistency calculations), 10 mRy, and 1 mRy (typical for density-of-states calculations).

Appendix

Real Spherical Harmonics

The real spherical harmonics Y_{lm} are defined by a unitary transformation of the (usual) complex spherical harmonics Y^c_{lm}:

$$Y_{lm} = \begin{cases} \frac{1}{\sqrt{2}}(Y^c_{lm} + Y^c_{l,-m}) & m > 0 \\ \\ Y^c_{l,0} & m = 0 \\ \\ \frac{-i}{\sqrt{2}}(Y^c_{l,|m|} - Y^c_{l,-|m|}) & m < 0. \end{cases} \tag{148}$$

The complex spherical harmonics are defined as

$$Y^c_{lm}(\theta,\phi) = (-1)^{(m+|m|)/2}\sqrt{\frac{2l+1}{4\pi}\frac{(l-|m|)!}{(l+m)!}}P_l^{|m|}(\cos\theta)e^{im\phi} \tag{149}$$

where $P_l^{|m|}(x)$ are the Legendre functions

$$P_l^{|m|}(x) = \frac{1}{2^l l!}(1-x^2)^{|m|/2}\frac{d^{l+|m|}}{dx^{l+|m|}}(x^2-1)^l. \tag{150}$$

References

1. J. Korringa, Physica **13**, 392 (1947).
2. W. Kohn and N. Rostoker, Phys. Rev. **94**, 1111 (1954).
3. T. H. Dupree, Ann. Phys. (N. Y.), **15**, 63 (1961); J. L. Beeby, Proc. Roy. Soc. London Ser. A**302**, 113 (1967); G. J. Morgan, Proc. Phys. Soc. **89**, 365 (1966).
4. For a review of the KKR method, see N. Papanikolaou, R. Zeller, and P. H. Dederichs, J. Phys.: Condens. Matter **14**, 2799 (2002).
5. R. Zeller and P. H. Dederichs, Phys. Rev. Lett. **42**, 1713 (1979).
6. I. Mertig, E. Mrosan, and P. Ziesche, *Multiple Scattering Theory of Point Defects in Metals: Electronic Properties*, Teubner-Texte zur Physik 11, Teubner Verlag Leibzig (1987).
7. For a comprehensive presentation of the KKR and KKR-CPA methods and many of their applications, see: A. Gonis, *Theoretical Materials Science*, Materials Research Society (2000).
8. R. Zeller, P. H. Dederichs, B. Újfalussy, L. Szunyogh, and P. Weinberger, Phys. Rev. B **52**, 8807 (1995); K. Wildberger, R. Zeller, and P. H. Dederichs, Phys. Rev. B **55**, 10074 (1997).
9. J. Banhart, H. Ebert, P. Weinberger, and J. Voitländer, Phys. Rev. B **50**, 2104 (1994); W. H. Butler, Phys. Rev. B **31**, 3260 (1995).
10. Ph. Mavropoulos, N. Papanikolaou, and P. H. Dederichs, Phys. Rev. B **69**, 125104 (2004).
11. J. Minar, L. Chioncel, A. Perlov, H. Ebert, M. I. Katsnelson, and A. I. Lichtenstein, Phys. Rev. B **72**, 045125 (2005).

12. M. Asato, A. Settels, T. Hoshino, T. Asada, S. Blügel, R. Zeller, and P. H. Dederichs, Phys. Rev. B **60**, 5202 (1999).
13. I. Galanakis, G. Bihlmayer, V. Bellini, N. Papanikolaou, R. Zeller, S. Blügel, and P.H. Dederichs, Europhys. Lett. **58**, 751 (2002).
14. M. Freyss, N. Papanikolaou, V. Bellini, R. Zeller, and P. H. Dederichs, Phys. Rev. B **66**, 014445 (2002).
15. B. Nonas, K. Wildberger, R. Zeller, P. H. Dederichs, and B. L. Gyorffy, Phys. Rev. B **57**, 84 (1998).
16. H. Ebert and S. Mankovsky, Phys. Rev. Lett. **90**, 077404 (2003).
17. Ph. Mavropoulos, O. Wunnicke, and P. H. Dederichs, Phys. Rev. B **66**, 024416 (2002).
18. N. Papanikolaou, J. Opitz, P. Zahn, and I. Mertig, Phys. Rev. B 66, 165441 (2002).
19. A. Vernes, H. Ebert, and J. Banhart, Phys. Rev. B **68**, 134404 (2003).
20. V. Popescu, H. Ebert, B. Nonas, and P. H. Dederichs, Phys. Rev. B 64, 184407 (2001).
21. N. Stefanou, V. Karathanos, and A. Modinos, J. Phys. Condens. Matter **4**, 7389 (1992).
22. I. E. Psarobas, N. Stefanou, and A. Modinos, Phys. Rev. B **62**, 278 (2000); R. Sainidou, N. Stefanou, and A. Modinos, Phys. Rev. B **69**, 064301 (2004).
23. A. Modinos, V. Yannopapas, and N. Stefanou, Phys. Rev. B **61**, 8099 (2000).
24. R. G. Newton, *Scattering Theory of Waves and Particles*, second edition, Springer (1982); reprint by Dover (2002).
25. E. N. Economou, *Green's functions in Quantum Physics*, Springer Series in Solid-State Sciences 7, Springer Verlag Berlin (1979).
26. G. Arfken, *Mathematical Methods for Physicists*, Academic Press International Edition (1970).
27. R. Zeller, J. Phys. C: Solid State Phys. **20** 2347 (1987).
28. B. Drittler, M. Weinert, R. Zeller, and P. H. Dederichs, Solid State Commun. **79**, 31 (1991).
29. N. Stefanou, H. Akai, and R. Zeller, Comp. Phys. Commun. **60**, 231 (1990); N. Stefanou and R. Zeller, J. Phys.: Condens. Matter **3**, 7599 (1991).
30. O. K. Andersen and O. Jepsen, Phys. Rev. Lett. **53**, 2571 (1984).
31. B. Wenzien, J. Kudrnovský, V. Drchal, and M. Šob, J. Phys.: Condens. Matter **1**, 9893 (1989).
32. J. Kudrnovský, V. Drchal, I. Turek, and P. Weinberger, Phys. Rev. B **50**, 16105 (1994).
33. K. Wildberger, P. Lang, R. Zeller, and P. H. Dederichs, Phys. Rev. B **52**, 11502 (1995).